Biosensors and Bioelectronics 28 (2011) 210–215

Contents lists available at ScienceDirect

Biosensors and Bioelectronics

journal homepage: www.elsevier.com/locate/bios

A novel electrochemical sensor surface for the detection of hydrogen peroxide using cyclic bisureas/gold nanoparticle composite

Manjusha Mathew, N. Sandhyarani*

Nanoscience Research Laboratory, School of Nano Science and Technology, National Institute of Technology Calicut, Calicut, Kerala, India

ARTICLE INFO

Article history:
Received 30 March 2011
Received in revised form 10 July 2011
Accepted 11 July 2011
Available online 20 July 2011

Keywords:
Cyclic bisureas
Hydrogen peroxide
Self-assembled monolayers
Electrochemical sensor
Cyclic voltammetry

ABSTRACT

A novel electrochemical sensor surface with enhanced sensitivity for the detection of hydrogen peroxide has been developed based on the layer-by-layer assembly of mercapto propionic acid (MPA), cystine-based polymethylene-bridged cyclic bisureas (CBU)/gold nanoparticle (AuNP) and horseradish peroxidase (HRP) on gold electrode. Possibility of a large number of hydrogen bonds, allowed by the chemical and sterical structure of the CBU ensures the proper immobilization of the enzyme in favorable orientation and retention of enzymatic activity. Efficient electron tunneling property of AuNP together with its electrocatalytic activity leads to higher sensitivity in the detection of H_2O_2. In cyclic voltammetry measurements a cathodic current due to direct electron transfer of HRP is observed which, indicates excellent electrocatalytic activity of the sensor surface. The biosensor surface modified with gold nanoparticle and CBU showed a lower detection limit of 50 nM for hydrogen peroxide. Chronoamperometry is performed at −0.3 V and Michaelis–Menten constant K_M^{app} value is estimated to be 4.5 μM. The newly developed sensor surface showed very high stability, reproducibility and high sensitivity.

1. Introduction

Nanotechnology plays an important role in the development of biosensors. Achieving higher sensitivity, selectivity, reproducibility and stability of the sensor surface being the major challenges in the development of biosensors. Of this the sensitivity and detection range are vital. Majority of the sensors operate through interaction of the surface parameters like surface area with analyte concentration. Hence the sensitivity is determined by the real surface area of the sensor that interacts with the analyte. Nanoparticles/nanomaterials provide a provision for increasing the surface area. Different nanostructured materials have been extensively used in the development of biosensors especially electrochemical sensors due to their unique stable physical and chemical properties owing to the small size (Nakamura and Karube, 2003). The stability and electrochemical characteristics of an enzymatic biosensor are determined by the enzyme immobilization as well as the electron transfer from enzyme to the transducer surface (Martin et al., 2007). Direct electron transfer of the redox enzyme with the electrode is complicated due to the deeply buried electroactive cofactor of the redox enzyme inside the insulated protein shells (Chunbo et al., 2005). The simple versatile self assembly technique can produce well-ordered, homogeneous and molecular dimensioned monolayers on the surface of electrode (Swalen et al., 1987), which can both facilitate electron transfer between the analyte and the electrode and reduce the non-Faradic background currents, offering good reproducibility and short response time (Xiao et al., 2000).

Among the widely used nanomaterials for the sensor applications, carbon nanotubes (Santhosh et al., 2006; Tripathi et al., 2006) gold nanowires (Xu et al., 2010), silicon nanowires (Shancheng et al., 2010), silver nanoparticles (Chunbo et al., 2005) and gold nanoparticles (Liu and Ju, 2002; Xi-Liang et al., 2005) have attracted more attention in the application of electrochemical sensors. Decoration of different nanostructured materials with gold nanoparticles increases their sensitivity because of their electrocatalytic activity and small size (Xiao et al., 1999; Wang and Erkan, 2004). Surface attachment properties of more biocompatible peptide nanotubes have also been used for the development of biosensors (Miri et al., 2005).

One of the important enzymatic sensor surface developed is for the detection of hydrogen peroxide. Sensitive and accurate measurement of H_2O_2 is of considerable interest as it is an essential mediator in biology, medicine (Forzani et al., 1995) and also an important byproduct of enzymatic oxidation of several highly selective oxidases. Hydrogen peroxide is necessary for the metabolism of proteins, carbohydrates, fats, vitamins etc. and also helps to regulate blood sugar and in cellular energy production (Xu et al., 2010). Oxidative damages in the body are caused by cellular imbalance of H_2O_2 as it plays an important role in cell signaling and communication (Dröge, 2002). The sensitivity in the detection of hydrogen peroxide is of high importance in analytical, biomedical and environmental chemistry too. Even though various analytical

* Corresponding author. Tel.: +91 495 2286537; fax: +91 495 2287250.
E-mail address: sandhya@nitc.ac.in (N. Sandhyarani).

0956-5663/$ – see front matter © 2011 Elsevier B.V. All rights reserved.
doi:10.1016/j.bios.2011.07.020

techniques like spectrophotometry (Matsubara et al., 1992), colorimetry and titrimetry have been employed for the determination of H_2O_2, voltammetric determination has been found to be promising as it has both intrinsic selectivity and sensitivity (Kafi et al., 2002; Feng et al., 2010; Razmi and Habibi, 2009). Mediators such as ferrocene derivatives (Schubert et al., 1991; Tatsuma et al., 1989) and some polymers (Vreeke et al., 1995) have been used to shuttle electrons between the enzyme and the electrode. Even though a higher sensitivity could be achieved by the use of mediators, contamination of the sample solution is a major drawback. Direct attachment of enzymes on naked metal surfaces can result in denaturation of the enzyme and loss of bioactivity; however, such proteins when adsorbed on the surface of metal nanoparticles retain their biological activities (Crumbliss et al., 1992).

In this work we have explored the combined effect of electrocatalytic activity and higher surface area of gold nanoparticles and biocompatibility of cystine-based polymethylene-bridged cyclic bisureas on the performance of an electrochemical biosensor surface towards the response to hydrogen peroxide. Cyclic bisureas owing to its large number of peptide groups can form hydrogen bonds with the hydrophilic amino acid residues, which prevail on the surface of enzyme. Cyclic bisureas protected gold nanoparticles have been prepared and assembled on the surface to produce a composite material with properties of high electrocatalytic activity and efficient immobilization of enzyme without affecting its activity. The work reported here is novel as it explores the possibility of the development of sensor surface by immobilization of enzyme through hydrogen bonding from cyclic bisureas. For the synthesis of cyclic bisureas–Au nanoparticle composite, CBU solution in methanol was mixed with glutamate protected gold nanoparticle and stirred overnight. The disulfide bond in the CBU binds with Au and forms a stable CBU–AuNP composite. This composite was put on the mercaptopropionic acid (MPA) monolayer surface on the gold electrode. Further horseradish peroxidase was immobilized on the surface. The Au/MPA/CBU–AuNP/HRP electrode (Electrode 2) shows enhanced sensitivity to H_2O_2 compared to the Au/MPA/CBU/HRP electrode (Electrode1) without gold nanoparticles. In addition, the analytical performance of the biosensor with respect to repeatability, selectivity and stability were also evaluated.

2. Experimental

2.1. Reagents and materials

Peroxidase from horseradish type V1-A, hydrogen tetrachloroaurate trihydrate, 1,6-diisocyanato hexane and L-cystine dimethyl ester dihydrochloride were obtained from Sigma–Aldrich. All other chemicals (monosodium glutamate, H_2O_2, Na_2CO_3, Na_2HPO_4, KH_2PO_4) were of analytical grade and used without further purification. The supporting electrolyte 0.1 M phosphate buffered saline buffer was prepared by mixing the stock solutions of 0.1 M Na_2HPO_4 and KH_2PO_4 and the pH was adjusted using NaOH or HCl. All solutions were prepared with ultrapure water obtained from an ultrafiltration system (18 MΩ cm, Milli-Q, Millipore system).

2.2. Apparatus

Cyclic voltammetric (CV) studies and amperometric measurements were performed with CH 400A Electrochemical Quartz Crystal Microbalance (CH Instruments, Austin, TX). The three electrode system comprising of a platinum wire as auxiliary electrode and saturated calomel as the reference electrode against which all potentials were measured and the modified gold electrode as working electrode were used for the CV measurements. Electrochemical measurements were carried out at room temperature with a scan rate of 100 mV/S. Quartz crystal microbalance (QCM) measurements were done by a CH 400A electrochemical quartz crystal microbalance with 8.9 MHz resonance frequency. QCM experiments were carried out on a gold disk electrode as a working electrode, calomel electrode as reference electrode and a platinum wire as counter electrode. Scanning Electron Microscope (SEM) images were obtained using Hitachi SU6600 Variable Pressure Field Emission Scanning Electron Microscope. Images were obtained at an accelerating voltage 20 kV. Atomic force microscopy (AFM) experiments were performed using Park XE-125 atomic force microscope. Typical AFM images were acquired in non contact mode with silicon nitride cantilever. All measurements were performed at room temperature.

2.3. Synthesis of 18-membered cyclic bisureas and CBU–AuNP composite

Hydrogen bonded self assembled cystine-based polymethylene-bridged cyclic bisureas was synthesized following a standard procedure (Ranganathan et al., 1999). Briefly, 10 mM L-cystine di-OMe dihydrochloride was mixed with an ice cold saturated solution of sodium carbonate and stirred for ~10 min at 0 °C. The pH of the solution was maintained at ~9. The clear solution was extracted with dichloromethane and dried. To the freshly generated cystine-based free base, 5 mM of 1,6-diisocyanato hexane was added drop wise and stirred at room temperature for 12 h. The solvents were evaporated and the residue was chromatographed over a column of silica gel using a chloroform/methanol mixture. Due to its large number of peptide bonds and higher possibility of hydrogen bonding, the bisureas rings align in a parallel fashion, stacked on one another leading to the formation of an open ended tube in the crystalline form but remain as independent rings in methanol solution. This feature attracted our attention and selected CBU as a potential candidate for the immobilization of enzyme through hydrogen bonding.

A homogeneous stock solution of CBU was prepared by dissolving 12 mg CBU in 25 mL methanol. 1.5 mL of stock solution was mixed with 5 mL of AuNP solution. For the synthesis of gold nanoparticles (Parvathy et al., in preparation), 4 mL of 0.19 mM $HAuCl_4$ was added to 100 mL distilled water and boiled. To the boiling solution 20 mL of 1.27 mM monosodium glutamate was added leading to the formation of gold nanoparticles. The synthesized nanoparticles showed plasmon peak at 526 nm. The mixture of CBU and AuNP is stirred at room temperature for 12 h to obtain the CBU–AuNP composite. It is theorized that in solution, the gold nanoparticles of size ~20 nm are capped with cyclic bisureas.

2.4. Fabrication of H_2O_2 biosensor

Before modification, the bare gold electrode was abraded with emery paper and polished to a mirror like surface with 0.3 μm α-Al_2O_3 slurry followed by rinsing with copious amount of deionized water. Then the electrode was immersed in a freshly prepared Piranha solution (3:1 mixture of conc. H_2SO_4 and 30% H_2O_2, CAUTION: Piranha solution reacts violently with organic matter and is extremely corrosive) for 10 min. After being sonicated with deionized water, the electrode was rinsed with ethanol and dried. Mercapto propionic acid monolayer was prepared by soaking a clean gold electrode in 1 mM mercapto propionic acid in ethanol for 12 h at room temperature. The electrode was thoroughly rinsed with copious amount of ethanol to remove the physically adsorbed thiol and dried. Then the electrode was placed into 1 mM CBU (Electrode 1) or CBU–AuNP (Electrode 2) composite in methanol for 4 h. Finally covalent attachment of HRP to the modified electrode was achieved by incubating the electrode in 1 mM HRP in PBS for 12 h

to realize the H_2O_2 sensor. After thoroughly rinsing the sensor with deionized water, it was kept at 4 °C when not in use. The preparation process of hydrogen peroxide sensor surface is shown in Fig. 1B.

3. Results and discussion

3.1. Characterization of electrode surface

3.1.1. Cyclic voltammetry

Cyclic voltametry of ferro/ferricyanide redox couple is a valuable and convenient tool to monitor the characteristic of the surface modified electrodes. Cyclic voltammetry was conducted in 5 mM $Fe(CN)_6^{3-/4-}$ and 0.1 M KCl at 100 mV s^{-1} for four different types of electrodes viz., bare Au, Au/MPA, Au/MPA/CBU–AuNP composite, Au/MPA/CBU-AuNP/HRP. Fig. 1 compares the voltammetric response at each stage of the fabrication process.

Bare gold electrode showed a large signal response towards the Fe^{2+}/Fe^{3+} redox couple. Self assembly of mercapto propionic acid on the electrode surface generated an insulating layer on the electrode that functioned as a barrier to the electron transfer between the Fe^{2+}/Fe^{3+} and electrode surface, leading to a reduction in anodic and cathodic current. The current obtained after CBU–AuNP nanocomposite immobilization showed a remarkable increase. The immobilization of gold nanoparticles onto the MPA modified electrode markedly promoted the electron transfer of the analyte and the electrode surface and hence increased the current response. Modification of the electrode surface with HRP monolayer further decreases the redox current values because of its insulating nature.

The effective surface area of enzyme modified electrode was estimated using $Fe(CN)_6^{3-/4-}$ redox couple (Fig. 1). According to Randles–Sevcik equation (Xu et al., 2010)

$$I_p = 2.69 \times 10^{-5} A n^{3/2} D_0^{1/2} \upsilon^{1/2} C_0$$

where I_p, A, n, D_0, υ and C_0 represent the redox peak current (A), the effective surface area of the electrode (cm^2), electrons per molecules oxidized or reduced ($n = 1$), diffusion coefficient of $K_3[Fe(CN)_6]$ in 0.1 M KCl (0.673×10^{-5} cm^2 s^{-1}), scan rate (V s^{-1}) and concentration of redox species (mol cm^{-3}). The effective surface area of CBU/HRP and CBU–AuNP/HRP electrodes was calculated to be 0.031 cm^2 and 0.036 cm^2, respectively. An increase in the surface area in the nanoparticle modified surface is attributed to the increased surface area of the immobilized nanoparticle, which paved the way for immobilization of larger number of HRP on the surface of the sensor.

3.1.2. Scanning electron microscopy

The modification of Au electrode at each stage was also monitored by scanning electron microscopy. The micrographs of the electrode at different modification steps are shown in Fig. 2. Significant difference in the morphology was observed during stepwise modification. The images A, B, C and D depict the typical morphology of Au, Au/MPA, Au/MPA/CBU–AuNP, Au/MPA/CBU–AuNP/HRP, respectively. The surface of bare Au was flat with some roughness as seen and by the formation of self assembled monolayers (SAMs) the surface became smooth. One can see that CBU/AuNP nanocomposite show compact sphere on the surface and regularly dispersed on the surface. Such surface increases the effective surface area for the immobilization of enzyme. When HRP was immobilized on the surface, the aggregates of enzyme molecules exhibited as island like structures.

3.1.3. Atomic force microscopy

Distribution of CBU–AuNP on the electrode is further monitored by AFM. The AFM images of gold electrode before and after modification with CBU–AuNP are taken (supplementary information Fig. 1). The gold surface is observed to be flat. After the immobilization of CBU–AuNP, the number of particles on the surface was increased remarkably, this in turn increases the effective surface area of the substrate electrode to load large amount of HRP. This effectively prevents the leaking of enzyme molecules from the biosensor.

3.1.4. Quartz crystal microbalance

The modifications achieved in the electrode by various immobilization steps are further confirmed by quartz crystal microbalance. The QCM is a well established method for the measurement of small changes in mass, based on the relationship between changes in mass of material attached to the crystal and the oscillation frequency of the crystal. A change in the resonant frequency can be recorded in response to the increase in mass of the crystal consequent to the adsorption of material on the electrode surface. The relationship between the changes in mass per unit area (Δm) and frequency (Δf) are given by Suerbrey equation (Suerbrey, 1959),

$$\Delta f = \frac{-2f_0^2}{A\sqrt{\mu\rho}} \Delta m$$

where Δf, f_0, Δm, A,μ and ρ represent the frequency change, resonance frequency of the fundamental mode (Hz), mass change (ng), area of the crystal (cm^2), shear modulus (g/cms^2) and density (g/cm^3) of the crystal, respectively. (Table 1 in supplementary information summarizes the quartz crystal frequency change and the mass adsorbed on the crystal surface after each step of immobilization).

It was evident from the QCM data that each layer deposition resulted in decrease in frequency and an increase in mass on the surface. The immobilization of thiol induces a shift in the frequency of about 15 Hz, which corresponds to the mass of 20.85 ng. The frequency shift was higher due to the immobilization of CBU–AuNP as expected, which indicate the deposition of a higher mass (136.22 ng) on the quartz crystal. Deposition of enzyme results in a frequency change of 27 Hz, corresponds to the deposition of 37.53 ng on the surface.

3.2. Electrocatalytic reduction of hydrogen peroxide

The electrocatalytic behavior of the modified electrode towards the electrochemical reduction of H_2O_2 was studied using cyclic voltammetry. Variation in response of electrodes viz. Au/MPA/CBU/HRP (Electrode 1) and Au/MPA/CBU–AuNP/HRP (Electrode 2) to the analyte was investigated. Electrochemical reduction of H_2O_2 with electrode 1 in 0.1 M PBS of pH 7.4 is shown in Fig. 3. A significant increase in the cathodic current was observed during the addition of 1 mM H_2O_2 to the PBS, which is taken as control, due to the reduction of H_2O_2 by HRP. The voltammetric response of Au/MPA/CBU/HRP electrode was not observed below 100 μM concentration of H_2O_2.

The enhancement in the sensitivity for the detection of hydrogen peroxide in the presence of gold nanoparticles is shown in Fig. 4. The sensitivity of the electrode for the detection of H_2O_2 has been increased more than 1000 fold with the presence of significant catalytic current even in the presence of 50 nM H_2O_2. An increase in reduction current has been observed with the increase in concentration of H_2O_2. A control experiment was performed both in presence and absence of enzyme, with 1 mM concentration of hydrogen peroxide to verify whether the catalytic current observed was due to the non enzymatic reduction of H_2O_2 or not. As shown in Fig. 4 inset, no catalytic current response to H_2O_2 was observed at the Au/MPA/CBU-AuNP electrode. From this it is concluded that the catalytic current was solely due to the HRP induced reduction of H_2O_2. This detection limit is lower than most of the reported

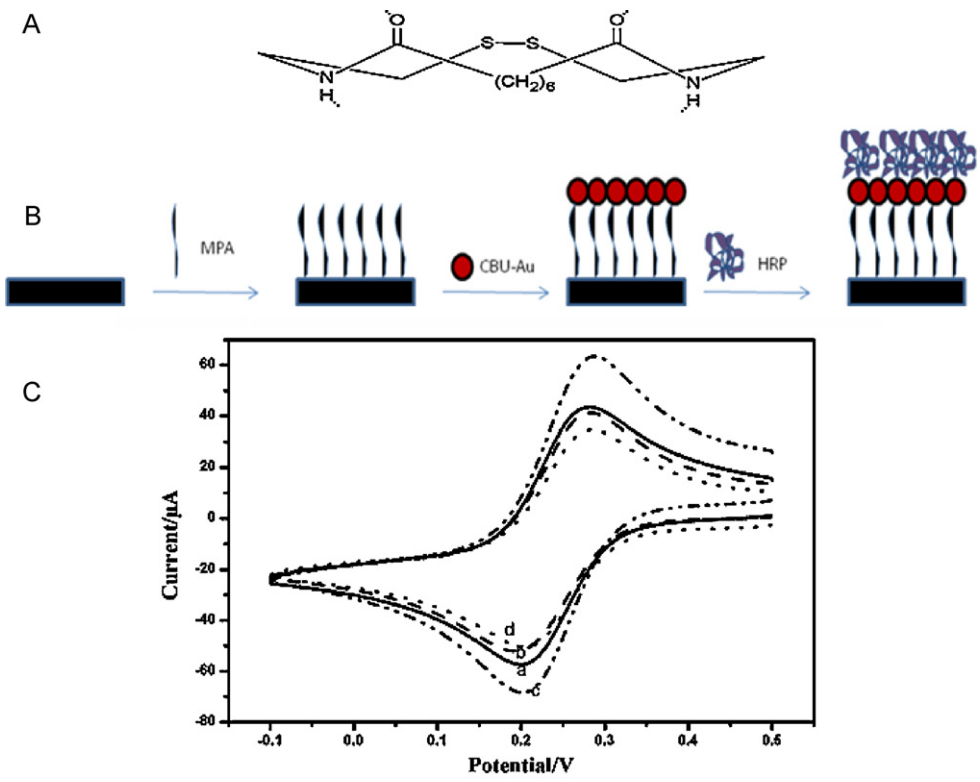

Fig. 1. (A) Structure of cyclic bisureas. (B) Schematic illustration of stepwise fabrication of the Au/MPA/CBU–AuNP/HRP modified electrode. (C) Cyclic voltammograms of (a) bare Au, (b) Au/MPA, (c) Au/MPA/CBU–AuNP, (d) Au/MPA/CBU–AuNP/HRP electrodes in 0.1 M KCl solution containing 5 mM $K_3[Fe(CN)_6]$.

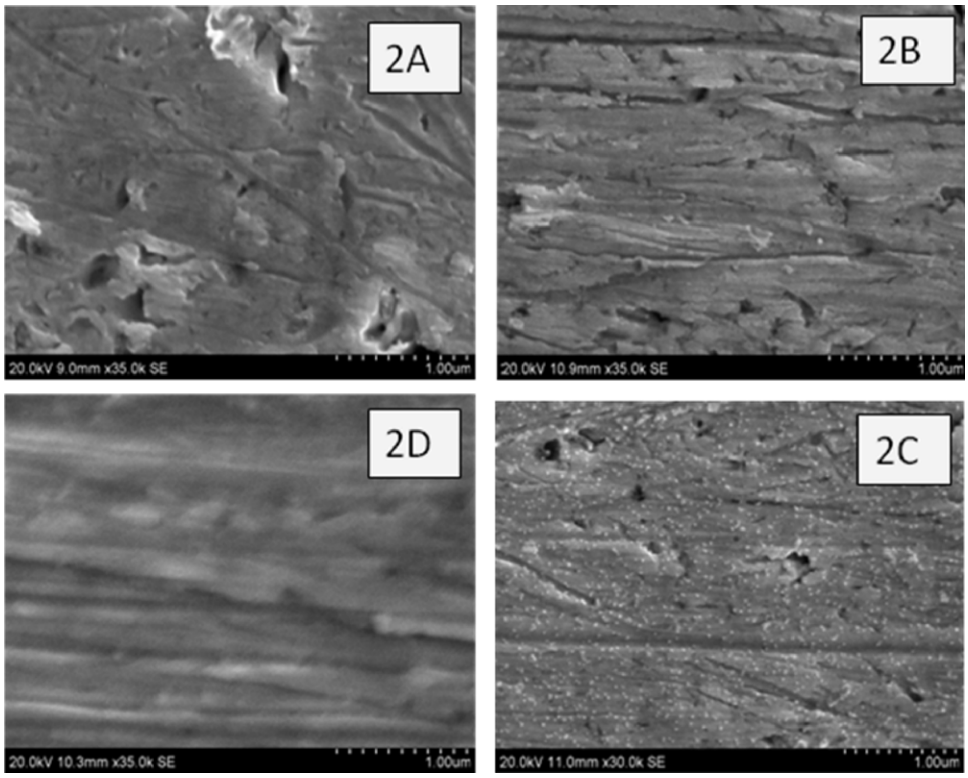

Fig. 2. SEM photographs of (A) Au, (B) Au/MPA, (C) Au/MPA/CBU–AuNP, and (D) Au/MPA/CBU–AuNP/HRP, respectively.

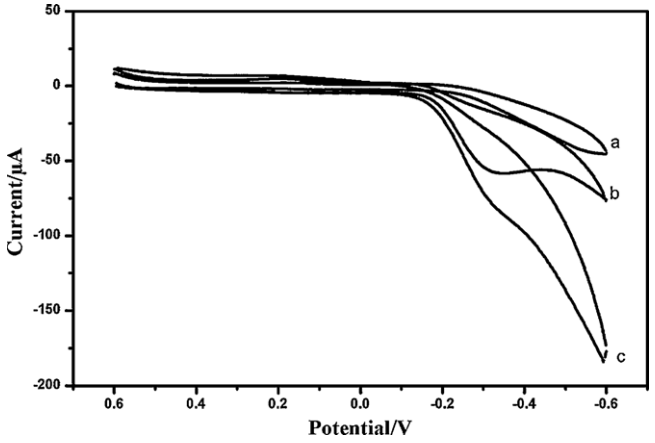

Fig. 3. Cyclic voltammogram of Au/MPA/CBU/HRP electrode in 0.1 M PBS (a) in the absence of H_2O_2 and in the presence of (b) 100 μM and (c) 1 mM H_2O_2.

value giving clear evidence for higher sensitivity of the electrode. Table 2 in supplementary information summarizes detection limit of different H_2O_2 biosensors.

The catalytic current obtained in both the electrode (Au/MPA/CBU/HRP and Au/MPA/CBU–AuNP/HRP) is due to the reduction of H_2O_2, which is explained as follows: H_2O_2 oxidizes the HRP–Fe(III) immobilized on the biosensor surface to form an intermediate which is a two equivalent oxidized form containing oxy ferryl heme (Fe^{4+}=O) and a porphyrin Π cation radical (compound 1). Porphyrin radical of compound 1 obtains one electron from the electrode to form a second intermediate (compound 2). Compound 2 is subsequently reduced back to native HRP by accepting one electron from the electrode. It is evident from the figure that as more H_2O_2 was added, the catalytic current increased, suggesting that the catalytic current was determined by the concentration of H_2O_2.

Gold nanoparticles present on the electrode surface can act as tiny conducting centers which allow efficient electron tunneling (Bharathi et al., 2001) and electron transfer between the enzyme and electrode surface (Zhao et al., 1992), enhancing the sensitivity of the sensor. The presence of gold nanoparticles on the electrode increases the surface area which subsequently acts as binding centers which increase the number of binding sites for HRP. Moreover, the gold nanoparticles modified with cyclic bisureas can provide a favorable micro environment for the active immobilization of HRP due to their biocompatibility and their hydrogen bonding capability.

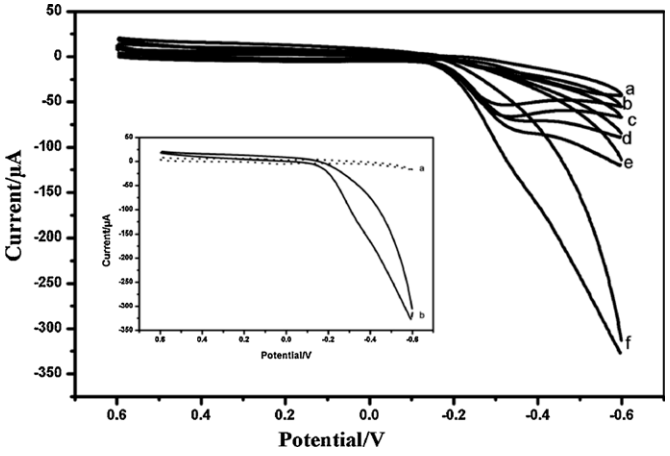

Fig. 4. Cyclic voltammogram of Au/MPA/CBU–AuNP/HRP modified electrode, (a) in the absence of H_2O_2. (b–f) Correspond to the cyclic voltammograms of the electrode in 50 nM, 100 nM, 10 μM, 100 μM and 1 mM of H_2O_2, respectively. Inset show CV of (a) Au/MPA/CBU–AuNP and (b) Au/MPA/CBU–AuNP/HRP electrode in 1 mM H_2O_2.

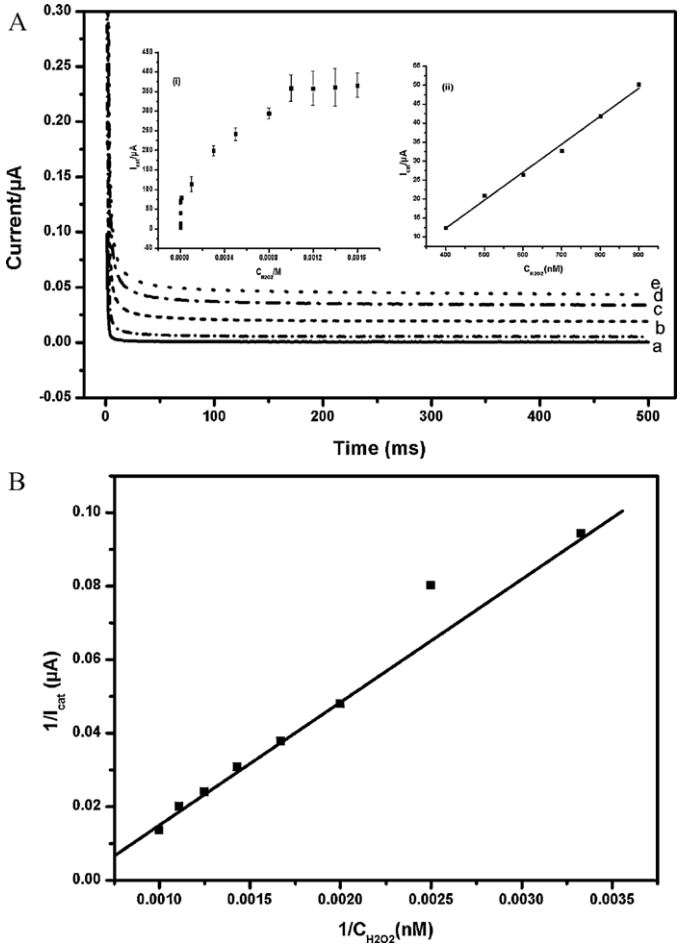

Fig. 5. (A) Chronoamperometric response of the Au/MPA/CBU-AuNP/HRP electrode at −0.3 V in unstirred PBS containing (a) 0, (b) 50, (c) 300 (d) 500 and (e) 800 nM H_2O_2. (Inset) (i) Plot of catalytic current vs. concentration of H_2O_2 and (ii) linear calibration curve and (B) Lineweaver–Burk plot of $1/I_{ss}$ vs. $1/C$.

3.3. Amperometric measurements and determination of Michaelis–Menten constant

Fig. 5 illustrates the chronoamperometric response of the Au/MPA/CBU–AuNP/HRP electrode with different concentrations of H_2O_2 in 0.1 M PBS at −0.3 V. In an unstirred solution, current decreases steeply to reach a stable value and the sensor achieve 95% of the steady state current within a few seconds (Huangxian and Donal, 1997; Song and Huang, 2002; Bingquan and Shaojun, 2000). With increase of H_2O_2 concentration, the current increases and a Michaelis–Menten type response is obtained at a concentration greater than 1 mM. The calibration range of H_2O_2 is 50 nM to 1.6 mM with a linear relation from 400 nM to 900 nM. This quick response is attributed to the fast electron transfer between the HRP and the gold sensing sites, due to the favorable orientation of HRP on Au nanoparticle.

The apparent Michaelis–Menten K_M^{app} constant, a reflection of both the enzymatic affinity and the ratio of microscopic kinetic constants, can be obtained from the electrochemical version of Lineweaver–Burk equation (Xiao et al., 2000). The K_M^{app} value for the Au/MPA/CBU–AuNP/HRP electrode is found to be 4.5 μM, which is significantly lower than the reported values (Xu et al., 2010). Though smaller values were reported (Anees et al., 2009) for K_M^{app},

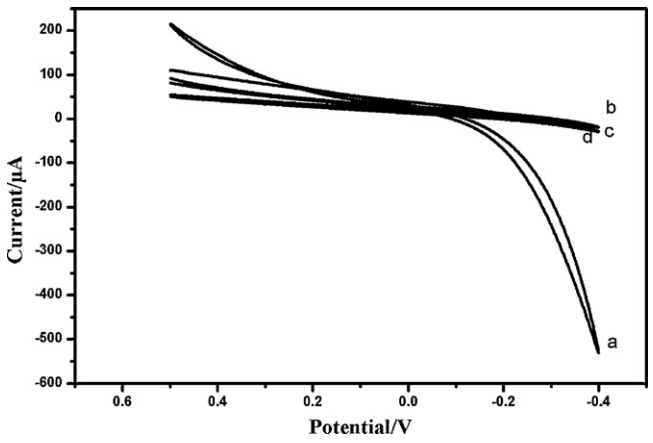

Fig. 6. Cyclic voltammetric response of the Au/MPA/CBU-AuNP/HRP modified electrode in presence of (a) 1 mM H_2O_2, (b) 1 mM glucose, (c) 1 mM BSA and (d) 1 mM ascorbic acid.

the sensitivity achieved in the present study is much higher when compared to the sensitivity of most of the previously reported sensor surfaces.

3.4. Selectivity, reproducibility and stability

The selectivity of the biosensor was evaluated by studying the interference of electro active compounds such as glucose, ascorbic acid and BSA. Fig. 6 shows the high selectivity of electrode surface to H_2O_2. It is seen that detectable current was observed only in presence of H_2O_2. Also the sensor surface gives unaffected analytical responses in presence of the interfering compounds.

Reproducibility of the biosensor was confirmed by preparing four electrodes independently and measuring the response for 1 μM H_2O_2 (Fig. 2 of supplementary information). All electrodes showed almost the same value of reduction current. The fabrication reproducibility for four sensor electrodes gave a relative standard deviation (RSD) of 6.4% for the determination of 1 μM H_2O_2. The good reproducibility may be due to the fact that the amount of CBU–AuNP composite was steady on the surface and HRP molecules were attached firmly onto the surface through hydrogen bonding without affecting its catalytic activity.

The stability of the H_2O_2 sensor surface was evaluated with its response to 50 nM H_2O_2 (Fig. 3supplementary information). When not in use, the electrode was stored at 4 °C. The response indicated that the sensitivity of the electrode remained relatively constant over four weeks of examination (The sensor surface retains 80% of its initial sensitivity after 30 days). Favorable microenvironment generated by the cyclic bisureas, maintaining the activity of HRP and preventing the leakage of the enzyme contributes highly to the stability of the electrode.

4. Conclusion

We have constructed a sensitive, selective, reproducible and low cost electrochemical H_2O_2 sensor by immobilizing HRP on a biocompatible self assembled Au/MPA/CBU–AuNP electrode. Nanomolar level sensitivity has been achieved by taking advantage of the electrocatalytic activity and efficient electron tunneling property of gold nanoparticles. The possibility of a large number of hydrogen bonds of the cyclic bisureas can account for its strong immobilization capacity, and retention of enzymatic activity of peroxidase. The sensor surface was highly robust, retaining its initial activity after 1 month storage at 4 °C. This provides a new strategy for the construction of an efficient H_2O_2 biosensor. To our knowledge this is the highest sensitivity achieved for the detection of hydrogen peroxide. In summary, rapid, simple, sensitive and cost effective detection of hydrogen peroxide can be achieved with the newly developed system and the proposed strategy can be extended for the development of other enzyme based biosensors.

Acknowledgements

Financial support from Department of Science and Technology, India is gratefully acknowledged. Authors thank Dr. C. Lakshmi, NIT Calicut for helpful discussions and valuable suggestions in cyclic bisureas synthesis. M.M. thanks CSIR, India for research fellowship.

Appendix A. Supplementary data

Supplementary data associated with this article can be found, in the online version, at doi:10.1016/j.bios.2011.07.020.

References

Anees, A.A., Pratima, S.R., Malhotra, B.D., 2009. J. Biotechnol. 142, 179–184.
Bharathi, S., Nogami, M., Ikeda, S., 2001. Langmuir 17, 1–4.
Bingquan, W., Shaojun, D., 2000. Talanta 51, 565–572.
Chunbo, R., Yonghai, S., Zhuang, L., 2005. Anal. Bioanal. Chem. 381, 1179–1185.
Crumbliss, A.L., Perine, S.C., Stonehuerner, J., Tubergen, K.R., Zhao, J., 1992. Biotechnol. Bioeng. 40, 483–490.
Dröge, W., 2002. Physiol. Rev. 81, 47–95.
Feng, L., Yan, F., Zhen, W., Limin, Y., Linhai, Z., Bo, T., 2010. Biosens. Bioelectron. 25, 2244–2248.
Forzani, E.S., Rivas, G.A., Solis, V.M., 1995. J. Electroanal. Chem. 382, 33–40.
Huangxian, J., Donal, L., 1997. Anal. Chim. Acta 345, 51–58.
Kafi, A., Guosheng, K.M., Aicheng, W.C., 2002. Biosens. Bioelectron. 24, 566–571.
Liu, S., Ju, H., 2002. Anal. Biochem. 307, 110–116.
Martin, P., Samuel, S., Izumi, I., Jie, T., 2007. Sens. Actuators, B 123, 1195–1205.
Matsubara, C., Kawamoto, N., Takamura, K., 1992. Analyst 117, 1781–1784.
Miri, Y., Meital, R., Ehud, G., Judith, R., 2005. Anal. Chem. 77, 5155–5159.
Nakamura, H., Karube, I., 2003. Anal. Bioanal. Chem. 377, 446–468.
Parvathy, R.C., Naseer, M., Udupa, N., Sandhyarani, N., in preparation.
Ranganathan, D., Lakshmi, C., Isabella, L.K., 1999. J. Am. Chem. Soc. 121, 6103–6107.
Razmi, H., Habibi, E., 2009. Anal. Biochem. 392, 126–132.
Santhosh, P., Manesha, K.M., Gopalan, A., Lee, K., 2006. Anal. Chim. Acta 575, 32–38.
Schubert, F., Saini, S., Turner, A.P.F., 1991. Anal. Chim. Acta 245, 133–138.
Shancheng, Y., He, N., Yinchen, S., Zhijuan, Z., Jiqing, Q., Zhongdang, X., 2010. J. Electroanal. Chem. 641, 136–140.
Song, Q., Huang, X., 2002. Anal. Biochem. 307, 110–116.
Suerbrey, G., 1959. Z. Phys. 155, 206.
Swalen, J.D., Allara, D.L., Andrade, J.D., Chandross, E.A., Graoff, S., Israelachvili, J., McCarthy, T.J., Murray, R., 1987. Langmuir 3, 932–950.
Tatsuma, T., Okawa, Y., Watanabe, T., 1989. Anal. Chem. 61, 2352–2356.
Tripathi, V.S., Kandimalla, V.B., Ju, H., 2006. Biosens. Bioelectron. 21, 1529–1535.
Vreeke, M., Rocca, P., Heller, A., 1995. Anal. Chem. 67, 303–306.
Wang, L., Erkan, W., 2004. Electrochem. Commun. 6, 225–229.
Xiao, Y., Huang, X.J., Hong, Y.C., 1999. Anal. Chim. Acta 391, 73–82.
Xiao, Y., Ju, H.X., Chen, H.Y., 2000. Anal. Biochem. 278, 22–28.
Xi-Liang, L., Jing, J.X., Qing, Z., Gong-Jun, Y., Hong, Y.C., 2005. Biosens. Bioelectron. 21, 190–196.
Xu, J., Shangb, F., John, H.T.L., Kafil, M.R., Jeremy, D.G., 2010. Biosens. Bioelectron. 25, 1313–1318.
Zhao, J., Henkens, R., Stonchuerner, T., O'Daly, J., Crunbliss, A., 1992. J. Electroanal. Chem 327, 109–119.